Research Article

Ruben Stahlbaum*, Lars Röhe, Martin Kleimeyer and Bert Günther

A generalised thermal LED-model and its applications

https://doi.org/10.1515/aot-2022-0017
Received April 22, 2022; accepted May 31, 2022;
published online June 30, 2022

Abstract: Within the last 10 years the illuminants for automotive exterior lighting shifted nearly completely to LEDs. Due to being semiconductor devices, LEDs behave differently compared to incandescent lamps and xenon bulbs. The paper derives a generalized thermal and geometric LED model. This gains advantage because the data provided in data sheets is different from manufacturer to manufacturer and even from one manufacturer the data is not standardized. So the data is not prepared to be included easily in any development process. In this context "model" mainly refers to a calculation procedure. The data provided in data sheets often has to be digitized. Outgoing from this digitized data a model, based on a smart data combination and polynomial regression, is built up. This model is described in detail and an application to simulations by means of computational fluid dynamics (CFD) is discussed. In doing so a geometric simplification is suggested. This simplification is done in a manner to keep the thermal characteristic of the original LED. The model may be used in different applications such as simulations and design. It allows predicting the thermal status and light output during a virtual development phase, because it inherently calculates the thermal power and light output. This may lead to a more precise estimation of temperatures in lighting systems as well as a prediction of hot lumens.

Keywords: CFD; colour shift; hot lumens; LED model; thermal degradation.

1 Introduction

Within the recent years there was a rapid change in the illuminants used for automotive exterior lighting applications. Nowadays light emitting diodes, LEDs, have become widely distributed as light sources instead of incandescent or Xenon bulbs. Whereas the latter illuminants have a more or less temperature independent light output, LEDs show degradation. This is a loss of lightflux when the LED is heated up or is operating at hot conditions. LEDs are also limited by the operating temperature in terms of damage and lifetime; see Colaco et al. [3]. On the other hand LEDs can be driven at different electric current to match thermal and optical requests. This needs to be considered in the design of lighting devices in order to fulfill design and legal requests.

Information to account for this is available in data sheets provided by LED manufacturers. The data sheets are divers in structure and information content. This makes it difficult to account for degradation in the development process as well as CFD simulations to predict thermal status and performance of a system, even if the importance of such simulations is pointed out by many groups e.g. [1, 3, 9]. It may be helpful to have a generalized LED model or calculation algorithm at hand, which is based on this data.

Keppens [4] proposed a model strategy based on fitting polynomials to current and temperature dependence of electrical power. The order of the polynomials were based on theoretical assumptions, and thus limited, including lots of parameters that are usually not available to the user. But he showed that it would be a valid procedure to combine the characteristics to get a two dimensional space of state. A good overview of actual model strategies is given by Poppe [8] who pointed out the importance of providing both junction temperature information and light output properties under application condition with different values of current.

Most of the suggestions are based on electronics simulation software like Spice or need parameters that are not easily available to everyone. We propose an approach to generalize the data provided by LED manufacturers via data sheets. Result is an algorithm that can predict thermal status and performance of LEDs by means of light output. A prediction of the colour shift is also possible. In Section 2 LEDs as light sources and their properties are described. This includes a brief discussion of how the data is given in

*Corresponding author: Ruben Stahlbaum, Volkswagen AG, Berliner Ring 2, 38440 Wolfsburg, Germany,
E-mail: ruben.stahlbaum@volkswagen.de
Lars Röhe, Martin Kleimeyer and Bert Günther, Volkswagen AG, Berliner Ring 2, 38440 Wolfsburg, Germany

data sheets. In Section 3 it is shown which information is necessary and how it may be combined in a general manner to form a model of the thermal behaviour of LEDs. In Section 4 the description of the calculation algorithm is given. Within a small example results of an implementation of the model into the CFD software Ansys Fluent by means of a user defined function are presented. A geometric simplification and generalization is suggested. This simplification is done in a way to keep the thermal characteristic, e.g. temperature distribution, of the original LED.

2 The LED

As semiconductor devices, LEDs emit light when electric current flows through their P–N-junction (see Kittel [5]). Herein the electrons combine with holes. The energy gained by this combination is released in form of photons of a more or less well defined distribution of wave lenghts, see Figure 1. The combination can be understood as electrons crossing the band gap formed by p- and n-regions. The colour is determined by the wavelengths of the emitted light. Red LEDs, for instance are called direct emitting. This means that the colour is given by the distribution of the emitted photons directly. White light in contrary cannot be emitted directly. In this case the LED is designed to emit blue light. Part of this light is converted by a layer of phosphorus into wide distribution of higher wave lengths with a peak at green light with $\lambda_{max} \approx 560$ nm. The mixture appears white to the human eye, see Section 2.2.

2.1 Luminous efficacy

Physically, the whole emitted light is called the radiant flux. The human eye is sensitive to only a certain part of a luminous spectrum. Its sensitivity to green light is used for daytime seeing. This is given by the luminous function, V_λ, with a maximum at $\lambda = 555$ nm, see the green dotted line in Figure 1. The luminous efficacy accounts for this selective sensitivity by measuring the fraction of light being visible to the human eye. Thus the radiant flux can be converted to light flux or luminous flux by convolving the spectrum with V_λ and integrating over all wavelengths within the interval of interest, which is typically from 380 to 780 nm. Radiant flux $\phi_{e,\,rel}$ is the amount of radiation emitted from the light source

$$\frac{\phi_e}{\phi_{e,\,typ}} = \phi_{e,\,rel} = \int_\lambda \phi_{e,\,rel}(\lambda)\,d\lambda$$

indicated as the red curve in Figure 1, whereas light flux $\phi_{v,\,rel}$ is radiant flux under consideration of the sensitivity of the human eye

$$\frac{\phi_v}{\phi_{v,\,typ}} = \phi_{v,\,rel} = K_m \int_\lambda \phi_{e,\,rel}(\lambda) V_\lambda d\lambda$$

represented by the orange curve. The photopic luminous efficacy, $K_m = 683\text{lm/W}$, is the conversion factor between radiant and luminous flux.

LEDs are usually characterised by light flux in lm. A significant amount of the electric power, P_{el}, is converted into radiation power, P_{opt}. The rest is dissipated as heat in form of thermal power, P_{th}, in the junction. The radiant efficiency or wall plug efficiency is the efficiency in which electrical power is being converted to optical power or radiation

$$\eta_{opt} = \frac{P_{opt}}{P_{el}}.$$

The optical power can be calculated by

$$P_{opt} = k_{rp} \cdot \Phi_V = \frac{\phi_{e,\,rel}}{\phi_{v,\,rel}} \cdot \Phi_V, \tag{1}$$

with the light flux Φ_V.

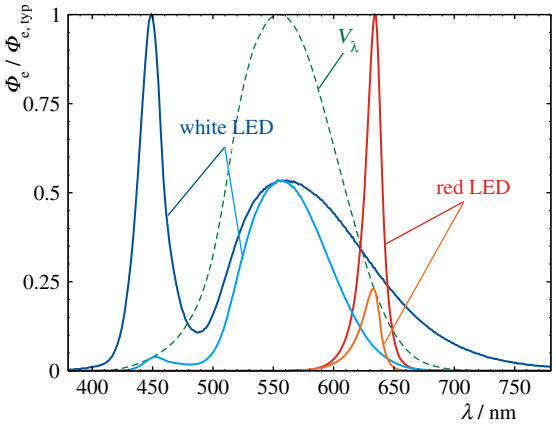

Figure 1: Normalised spectra of LEDs of different colour.

2.2 Colour according to CIE colour space

The colour of the emitted light is directly connected to its spectrum and the sensitivities of the three receptors in the human eye.

How can the colour be obtained from the spectrum? The essence of the calculation of a colour in CIE colour space using a luminous spectrum according to Ohno [7] is given in the following. According to CIE there exist three primaries, R/G/B, representing the wave length dependent colour sensitivity of the eye for monochromatic light of the

wavelengths 435.8 nm (blue light), 546.1 nm (green light) and 700 nm (red light). These primaries are called colour matching functions. CIE transformed them into another set of primaries which are denoted as CIE 1931 *xyz* colour matching functions, $\bar{x}(\lambda)$, $\bar{y}(\lambda)$ and $\bar{z}(\lambda)$, see Figure 2. The colour matching functions are then used to specify a light stimulus $\phi(\lambda)$ of any spectral distribution by convolving the spectrum with the colour matching function as in equations (2), (3) and (4). The result is called tristimulus values X, Y and Z, where

$$X = k \cdot \int_{380\text{nm}}^{780\text{nm}} \phi(\lambda) \cdot \bar{x}(\lambda) d\lambda, \tag{2}$$

$$Y = k \cdot \int_{380\text{nm}}^{780\text{nm}} \phi(\lambda) \cdot \bar{y}(\lambda) d\lambda, \tag{3}$$

$$Z = k \cdot \int_{380\text{nm}}^{780\text{nm}} \phi(\lambda) \cdot \bar{z}(\lambda) d\lambda, \tag{4}$$

and k is a normalizing constant.

The projection of the tristimulus values onto the unit plane $X + Y + Z = 1$ allows for displaying the colour in a two dimensional diagram, see Figure 3. The colour is then given by chromaticity coordinates x and y, equations (5) and (6).

$$x = \frac{X}{X + Y + Z} \tag{5}$$

$$y = \frac{Y}{X + Y + Z} \tag{6}$$

In automotive applications not all colours are allowed. There are usually legal regions given in which the colour of a given function has to be. This is added to the chromaticity diagram for white, yellow, orange and red as they are defined by ECE, for example.

2.3 LED characteristics

LEDs are characterized by manufacturers in order to enable the user to calculate all necessary values to describe optical and thermal behaviour. The data is based on measurements. As mentioned, there is a dependency on driving current and temperature which spans a huge two-dimensional space of measurements to be done. Manufacturers usually conduct two sets of measurement, one at fixed electric current and one at fixed temperature. The fixed values are denoted as typical and used to present the result in a dimensionless form. Usually the given temperature characteristics are based on the junction temperature, which is not easy to measure. For example T3STER technology provides one method for measurement, which according to Lee et al. [6], gives good results, but is rather time consuming. Another newly proposed method from Choi et al. [2], uses IR measurements of the phosphorus layer to determine the junction temperature by a linear correlation. However, to measure the temperature characteristics the manufacturers use a method with a very short measurement time, which ensures that the junction is not heated up during the measurement, so the ambient temperature and the junction temperature is the same. In applications the junction temperature is not known and the methods from above are generally not useable. What is usually measureable is the case point temperature. This is thermally connected to the junction temperature by the thermal resistance, see Section 4.1.

2.3.1 Data sheets

The LED data is provided in form of data sheets. These data sheets contain important constants, like minimum, maximum and typical values. Also included are graphs,

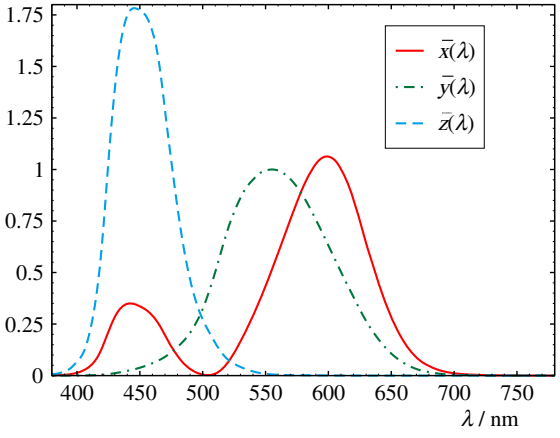

Figure 2: Colour matching functions according to CIE.

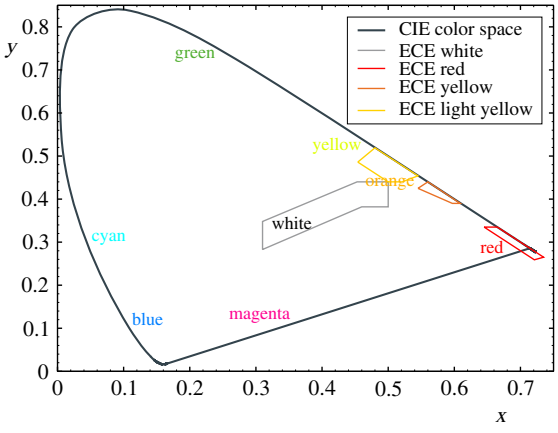

Figure 3: CIE colour space (chromaticity diagram).

showing the dependence of voltage, light flux and colour on temperature and electric current. Value groups and binnings are given as information on the range of performance for a specific LED.

Typical values are used to characterize a LED in terms of optical and thermal performance. They usually include

- typical forward current, $I_{F,\,typ}$,
- typical forward voltage, $U_{F,\,typ}$,
- typical temperature, $T_{j,\,typ}$,
- typical light flux, $\Phi_{v,\,typ}$,
- thermal resistance, R_{th}.

For the LED manufacturers these typical values are a degree of freedom to technically describe a LED in a data sheet. Also the way of presenting other details varies from manufacturer to manufacturer, also to point out different natures of the specific LEDs, like described above.

In Section 3 a generalized model for LEDs is derived to overcome these degrees of freedom and to enable comparisons of different LEDs in an easy way. The quality of the measurements inside the data sheets will not be further tested within the presented framework in this article. It has to be pointed out that the data provided by the manufacturers is of different quality, for an overview we refer to Keppens [4]. However, using the provided characteristics in a general model is the best one can do without own measurements and it improves CFD results a lot like it is shown in Section 4.6. In the upcoming sections an example set of characteristic data curves are described as a central point of the usual data sheets. All diagrams are given in dimensionless form for the discussion in this paper. Dots indicate measured points taken from data sheets.

2.3.2 Electric characteristics

The I–U-characteristic of an idealized LED is an exponential function of forward current I_F on forward voltage U_F, see Section 6.2.1. An example is given in the upper left of Figure 4.

The temperature dependence of the forward voltage is also provided as a graph, see the upper right of Figure 4 for the same LED. The voltage difference, $\Delta U_F = U_F - U_{F,\,typ}$, is based on a typical voltage, $U_{F,\,typ}$ given at the typical temperature $T_{j,\,typ}$.

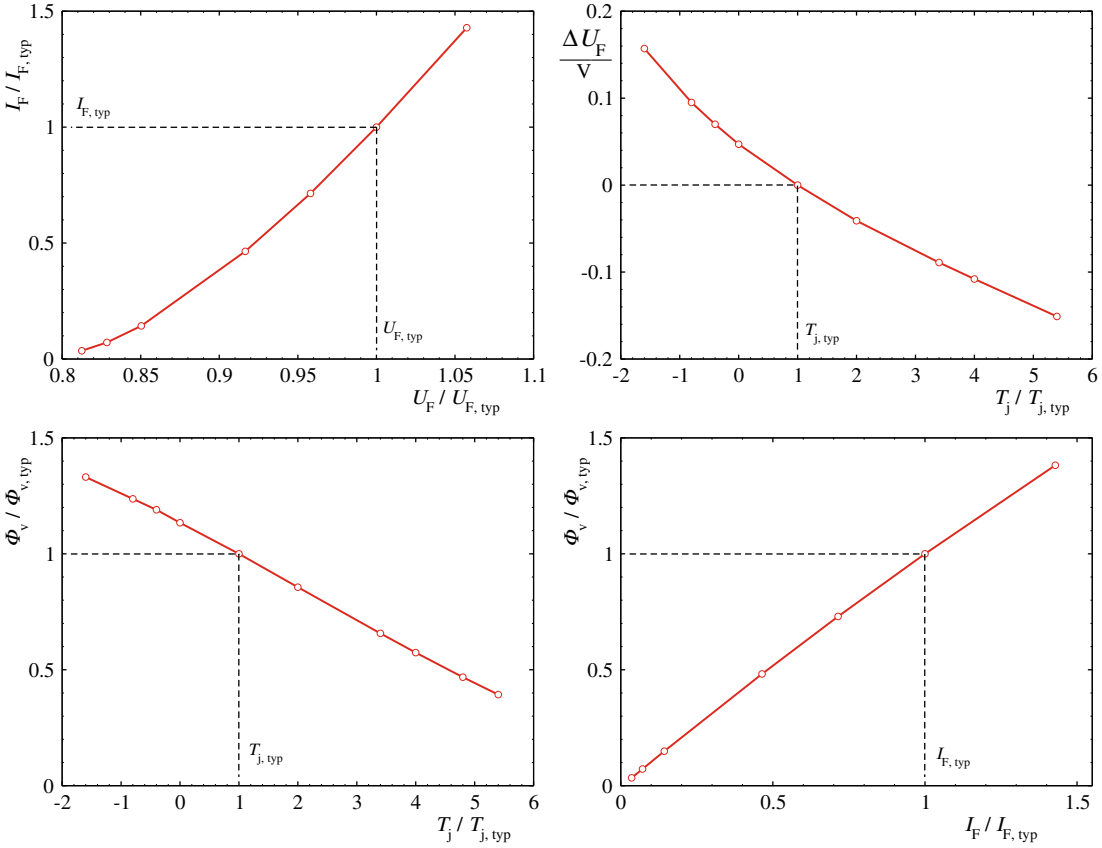

Figure 4: Usual LED characteristics given by data sheets. Normalized *I-U*-characteristic in the upper left and voltage shift due to temperature changes in the upper right. Relative light flux due to changes in junction temperature in the lower left and due to changes in forward current in the lower right.

2.3.3 Luminous characteristics

The dimensionless light flux Φ_{rel} is provided depending on temperature, $\Phi_{rel}(T_j, I_{F,\ typ})$ see lower left of Figure 4, and on forward current, $\Phi_{rel}(T_{j,\ typ}, I_F)$ see lower right of Figure 4. The dependencies appear to be more or less linear according to Keppens [4].

2.3.4 Colour characteristics

For different technologies the colour shift of LEDs due to temperature change is given by a shift of the dominant wavelength. It can be found in the literature (see Kittel [5]) linear relations of $\Delta\lambda_{dom} = 0.018\text{nm/K}$ for AlInGaP (yellow and red) and $\Delta\lambda_{dom} = -0.016\text{nm/K}$ for InGaN (blue, green and white). Often white LEDs generate their colour by a conversion of part of the emitted blue light by layer of phosphorus. In such case the simple relation cannot be used anymore. Additionally the dependence of the colour on the forward current would not be taken into account. Thus the authors decided to rely on the graphs given by the data sheets.

For directly radiating LEDs there is a luminous spectrum or the dominant wave length provided. The colour can be calculated according to Section 2.2. It changes mainly with changing temperature, described by a shift of the dominant wave length of the spectrum. Data sheets provide an according graph, see Figure 5.

For LEDs whose colour is produced by conversion, data sheets usually provide the colour change as coordinate changes in the chromaticity diagram, see Figure 3. There will also be a change due to current variation, as well as temperature variation, see Figure 6.

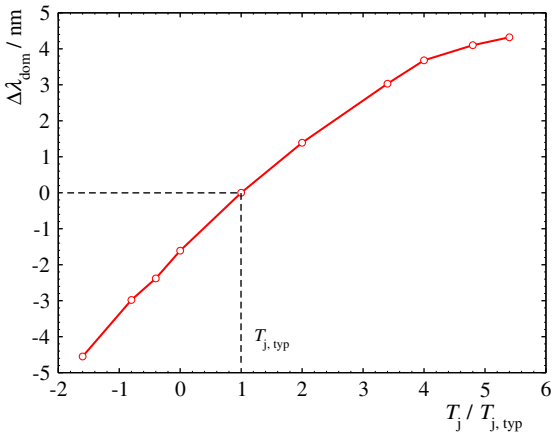

Figure 5: Temperature dependence of the dominant wave length.

2.3.5 Bins

The production process of LEDs is a rather complex task. This results in a statistical variance of the quality. To account for this, LEDs are grouped by means of bins. Bins form groups of the same characteristic within an interval. Characteristics with bins are forward voltage, luminance and colour or wave length.

As an example, brightness bins group the luminous flux of LEDs and are usually provided as tables containing the name, minimal and maximal flux. Sometimes a luminous intensity is given for minimum and maximum together with luminous flux for typical value or mean of the bin. The other technical quantities are presented accordingly.

3 LED-model

This section will propose a procedure for building a generalized model for thermal behaviour of LEDs based on the data described in Section 2.

In the following discussion we assume the data, especially the provided graphs, of the data sheet to be available in numerical form.

3.1 Space of the characteristics

3.1.1 Electrical power

There is a dependency of the I–U-characteristic on temperature as described in Section 2.3.2. The characteristic line will be shifted along the U_F-axis with varying temperature outgoing from the typical value $T_{j,\ typ}$ making use of the information given in the upper left of Figure 7. If we imagine a third axis of temperature perpendicular to the U_F–I_F-plane, the lines of the plot will form the black surface shown in the upper right of Figure 7. Thus U_F can be seen as a function of I_F and T_j,

$$U_F = f(T_j, I_F).$$

3.1.2 Luminousity

The relative light flux also shows a dependence of the two quantities I_F and T_j as described in Section 2.3.3, and illustrated in the lower row of Figure 4. The curves intersect at the typical point where the relative light flux is one. We can consider the curves to be independent from each other and being connected at the typical point at $\Phi_{rel} = 1$. By

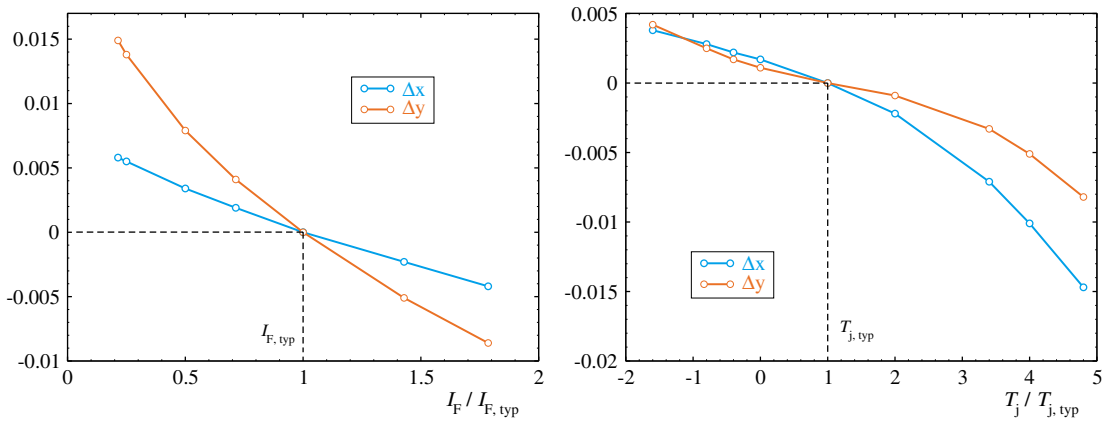

Figure 6: Forward current dependence (left) and junction temperature dependence (right) of the *x* and *y* colour coordinates.

shifting the curve dependent on the forward current along the one dependent on the junction temperature in the lower row of Figure 4 we get the set of curves given in the lower left of Figure 7. These curves can again be combined to a two dimensional surface over the T_j–I_F-plane, like it is illustrated in the lower right,

$$\frac{\Phi_v}{\Phi_{v,\,typ}} = f(T_j, I_F).$$

3.1.3 Colour

Description of colour shift due to temperature change requires differentiation between direct emitting and converted LEDs, as mentioned in Section 2.2.

Given a converted LED one can follow the procedure described for electrical power and luminosity combining the graphs in Figure 6 to get the black surfaces in Figure 8.

For direct emitting LEDs the shift of the dominant wave length with respect to temperature change is given. Therefore, one can only account for temperature dependence. The spectrum needs to be shifted according to the wave length shift, see Figure 5, and the resulting colour has to be calculated according to Section 2.2.

3.2 Regression functions

As seen in Section 3.1 there are dependencies of the characteristics which can be combined to form a surface. To make use of this description the data needs to be further processed. We chose a way to have the data approximated well with a minimum of parameters and error – two dimensional polynomial regression of limited order, see Appendix 6.1. A maximal $\mathcal{O}(5)$ would give a smooth approximation within the definition interval. The regression functions have the following form

$$U_F(T_j, I_F) \approx \sum_{i=0}^{n} \sum_{k=0}^{m} c_{U,ik} \cdot T_j^i \cdot I_F^k \tag{7}$$

$$\Phi_{rel}(T_j, I_F) \approx \sum_{i=0}^{n} \sum_{k=0}^{m} c_{\Phi,ik} \cdot T_j^i \cdot I_F^k \tag{8}$$

$$\Delta x(T_j, I_F) \approx \sum_{i=0}^{n} \sum_{k=0}^{m} c_{\Delta x,ik} \cdot T_j^i \cdot I_F^k \tag{9}$$

$$\Delta y(T_j, I_F) \approx \sum_{i=0}^{n} \sum_{k=0}^{m} c_{\Delta y,ik} \cdot T_j^i \cdot I_F^k \tag{10}$$

with n and m being the order of regression and (c_U), (c_Φ), $(c_{\Delta x})$ and $(c_{\Delta y})$ the matrices of regression coefficients. The order n and m of the polynomial should be chosen as low as possible and can be different in the two directions. As a remark we want to emphasize, that two characteristic curves are not enough to do a regression as smooth as in the figures above. For the presented regression the amount of data points was enhanced by superposition in the regression domain.

3.3 Extrapolations

Regression can only be done within the interval of data, i.e. the black area in the three dimensional plots in Figures 7 and 8. Polynomials of higher order tend to oscillate outside the definition area and will give unphysical results. But if temperature or current outside this interval is used or reached there still shall exist a physically appropriate solution, e.g., within a CFD simulation like in Section 4.6. Thus an extrapolation will be necessary.

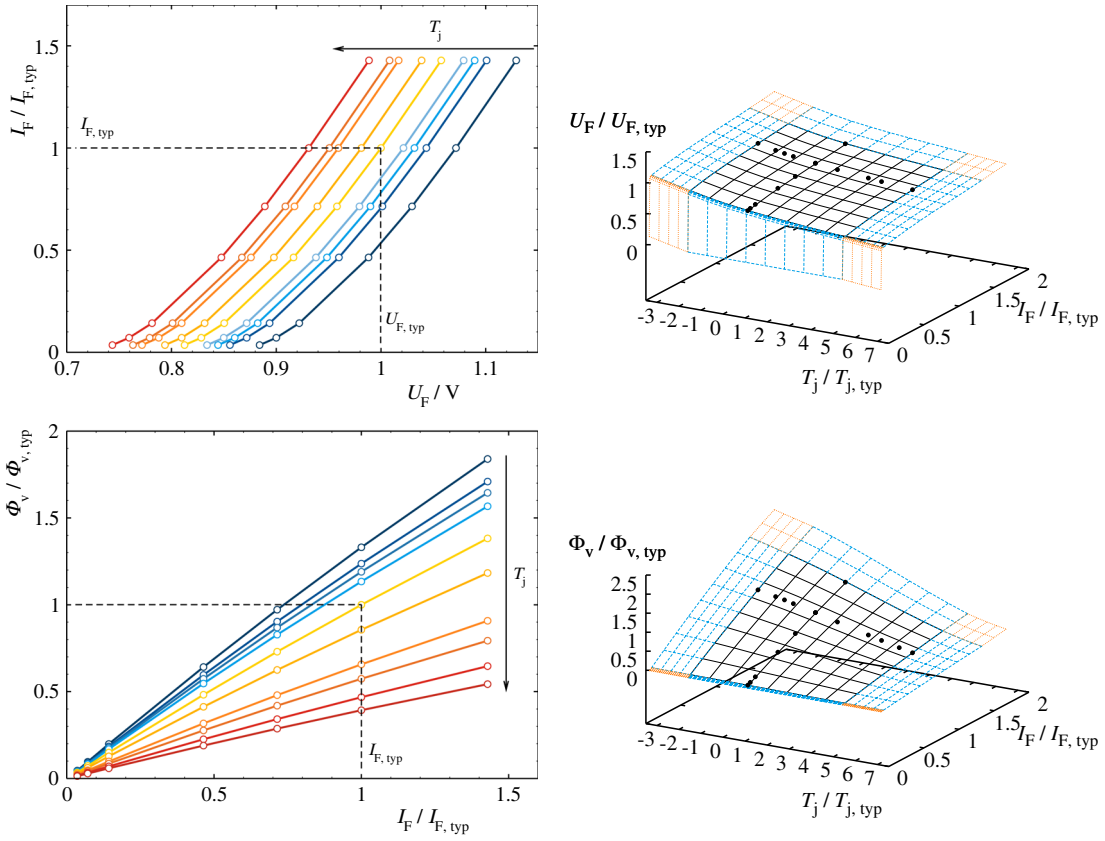

Figure 7: Temperature dependence of the *I*–*U*-characteristic and the forward voltage as a function of forward current and junction temperature in the upper row. Temperature dependence of the relative light flux over forward current and the relative light flux as a function of forward current and junction temperature in the lower row.

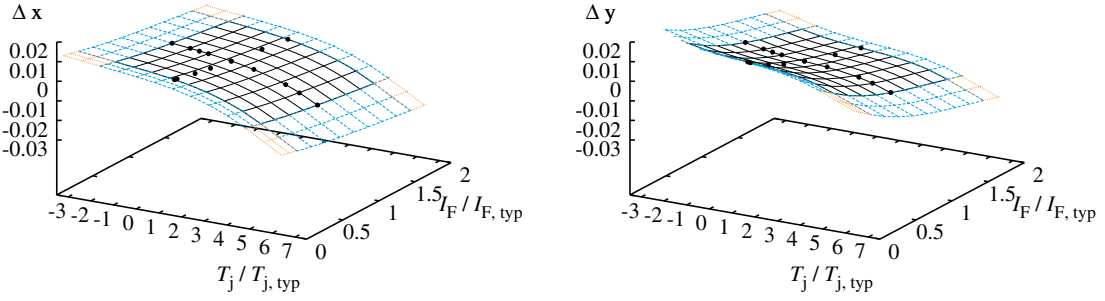

Figure 8: Δ*x* and Δ*y* as a function of forward current and junction temperature.

Let Ω be the domain of definition for the functions of interest according to equations (7) to (10).

Around the rectangular area Ω there appear eight regions as can be seen in Figure 9. The vertical and horizontal parts Ω_T-, Ω_T+, Ω_I- and Ω_I+ directly connect to the regression function and are extrapolations of the polynomials whereas the diagonal regions Ω_{--}, Ω_{-+}, Ω_{++} and Ω_{+-} are superposition of the bounding extrapolations.

The extrapolation functions are chosen such that the extension of the regression area will be physical. Our choice is explained in the appendix in Section 6.2.3.

4 Application of the LED-model

This section shows some of the benefits of our generalized approach. Not only can the regressions be used to calculate any values given by the regression functions and their

Ω_{-+}	Ω_{T+}	Ω_{++}
Ω_{I-}	Ω	Ω_{I+}
Ω_{--}	Ω_{T-}	Ω_{+-}

Figure 9: Extrapolation outside regression function.

extrapolation but it is also possible to calculate LED efficiency and other properties of importance.

4.1 Geometric LED-model

The geometry of LEDs can be rather complex consisting of a die, which contains the P-N-junction, electric and thermal connections, housing or mold compound and in some cases a phosphorus layer, see left plot of Figure 10. The exact internal geometry is often not available. Some LEDs are also very small, which makes it impractical to be spacially resolved within CFD simulations.

Fortunately, data sheets provide the thermal resistance, which connects the temperature of solder and junction if the thermal power is known,

$$T_\mathrm{j} = T_\mathrm{s}\left(T_\mathrm{j}, I_\mathrm{F}\right) + R_\mathrm{th} \cdot P_\mathrm{th}\left(T_\mathrm{j}, I_\mathrm{F}\right). \tag{11}$$

In CFD simulations, it would be necessary to know the exact geometry and all material properties for a certain LED. The manufacturers only seldom provide this information. Even if provided Yang et al. [12] showed that the geometry inside a real LED deviates from the perfect CAD-geometry and results therefore in different temperatures in simulation and measurement. Also the geometric model would be rather complex with the need of a very fine mesh. The thermal resistance provides the opportunity to create a simplified model as shown on the right in Figure 10 in a similar section, keeping a realistic temperature difference between junction and solder. To do so the outer shape is used as well as the position and shape of the die and the connections to the PCB, especially the solder point. The electrodes are neglected. This significantly changes the thermal resistance between junction and solder. To account for a correction a thin layer with adjustable thermal conductivity is implemented between die and mold compound. This allows an adjustment of R_th by changing the thermal conductivity of this additional layer. In order to generalize the geometric model the described simplifications will be applied to all LED types and the combinations of mold compound and electrical and thermal wiring are condensed into the R_th layer. The authors are aware that neglecting the thermal capacity of the different LED components by this simplification change the temporal response but considering the size of heat sinks and PCBs compared with the LED it will be acceptable from a system point of view for a lot of applictions.

4.2 Use of the regressions

The regression and extrapolations can be used to calculate the electric and photometric status of the LED depending on current and junction temperature as explained in Section 3. Colour shift is also directly accessible.

4.3 Expansion to other values

The thermal LED model presented in Section 3 provides the possibility to approximate the light flux Φ_V and the forward

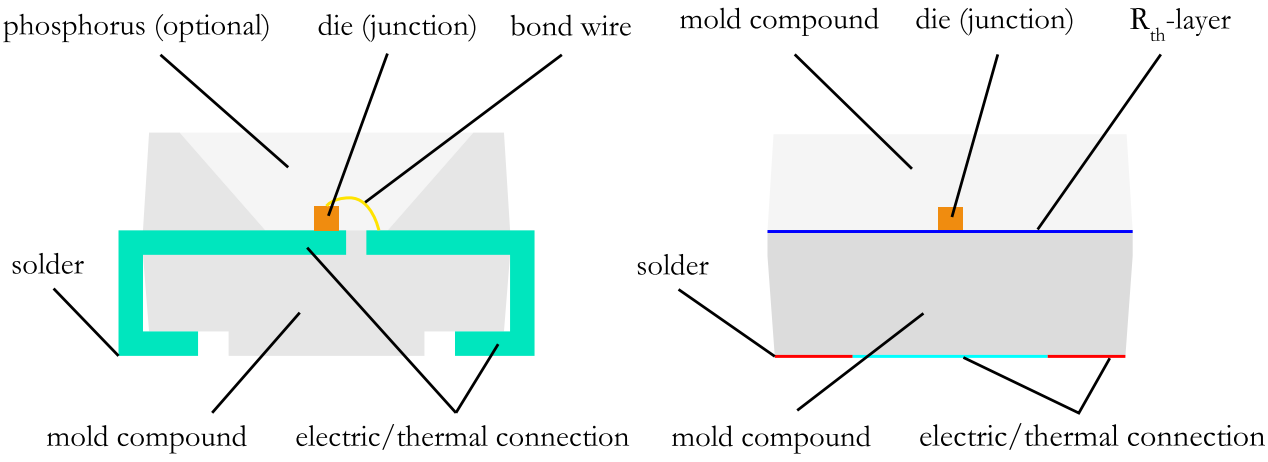

Figure 10: Section through typical low power LED on the left and section through the simplified geometrical model on the right.

voltage U_F as well as colour shift of a LED at any given junction temperature T_j and forward current I_F. With these values it is also possible to approximate other values of interest. The electrical, optical and thermal power can be calculated by

$$P_{el}(T_j, I_F) = U_F(T_j, I_F) \cdot I_F, \tag{12}$$

$$P_{opt}(T_j, I_F) = k_{rp} \cdot \Phi_V(T_j, I_F), \tag{13}$$

$$P_{th}(T_j, I_F) = P_{el}(T_j, I_F) - P_{opt}(T_j, I_F), \tag{14}$$

where Equation (1) is used. The radiant or wall plug efficiency and the thermal efficiency are given by

$$\eta_{opt}(T_j, I_F) = \frac{P_{opt}(T_j, I_F)}{P_{el}(T_j, I_F)}, \tag{15}$$

$$\eta_{th}(T_j, I_F) = \frac{P_{th}(T_j, I_F)}{P_{el}(T_j, I_F)} = 1 - \eta_{opt}(T_j, I_F).$$

Up to now, the temperature dependence of every value is with respect to the junction point at the die; see left side of Figure 10. This junction temperature T_j is hard if not impossible to be measured, since the P–N junction is not accessible. Measures of the temperature are often given at the solder or case point, Section 4.1, and between these two temperatures one can derive a connection with the thermal power and the thermal resistance according to equation (11). The thermal resistance is given in the LED data sheet by the LED manufacturer directly. The thermal resistance is assumed to be constant for simplicity, even if the authors are aware that this value might vary.

There are two different ways to look at the resistance of a LED. On the one hand we already used the real thermal resistance from the data sheet. On the other hand we can derive the electrical thermal resistance by using the radiant or optical efficiency, i.e.

$$R_{th,el}(T_j, I_F) = R_{th} - \eta_{opt}(T_j, I_F) \cdot R_{th} = \frac{T_j - T_s(T_j, I_F)}{P_{el}(T_j, I_F)}.$$

While the thermal resistance takes into account the dissipated thermal power, the electrical thermal resistance is defined with the supplied electrical power.

4.4 Driving a LED

LEDs are usually driven by current not by voltage. It is due to the exponential dependence of current on voltage. Thus a small change in voltage would result in a rather big change in current.

There are two different ways – by a constant forward current or by pulsed forward current. The latter is referred to as PWM or pulse width modulation. PWM usually runs at a high frequency, e.g. 200 Hz or more. So for any simulation it should be approximated by means of effective values instead of momentarily ones. On the other hand some lighting functions are operating in unsteady mode, e.g. turn indicator. In this case, for a stationary simulation, it will be necessary to modulate again with a duty cycle or switching rhythm. Consider the modulation to be of rectangular shape. In this case one can assume the period to have a length of time T with a temporal fraction τ where the signal is on. Thus any effective value will be a function of $f_{PWM} = \tau/T$, and the corresponding factor representing the duty cycle f_{cycle}. For forward current and forward voltage one will find that

$$I_{F,\,eff} = \sqrt{f_{cycle} f_{PWM}} \cdot I_F \tag{16}$$

$$U_{F,\,eff} = \sqrt{f_{cycle} f_{PWM}} \cdot U_F. \tag{17}$$

Combining equations (16) and (17) one finds that the effective electrical power becomes

$$P_{el,\,eff} = f_{cycle} f_{PWM} \cdot P_{el},$$

as does the thermal power

$$P_{th,\,eff} = f_{cycle} f_{PWM} \cdot P_{th}. \tag{18}$$

Similarly, for the effective light flux we obtain

$$\Phi_{v,\,eff} = f_{PWM} \cdot \Phi_v,$$

since the light flux is driven by the optical power. Note, the effective light flux $\Phi_{v,\,eff}$ does not depend upon the duty cycle, since the modulation of the duty cycle can be resolved by humans vision, e.g. turn indicator.

4.5 Calculation procedure in CFD

This section presents an algorithm to enable the engineer to easily calculate the complete thermal status of a LED as described in Sections 4.2, 4.3 and 4.4. This can be done explicitly or within a CFD simulation by means of user code.

The geometric model comprises the die as volumetric heat source, see right side of Figure 10. Due to having a small die volume compared to a LED, the mean temperature of it can be assumed to be T_j. The solder point T_s is also defined in the model. Thus the solder temperature can be read out as mean temperature of a tiny surface during the

calculation. This allows adjusting the thermal power of the LED and thus the heat source for the CFD simulation according to the current thermal status.

The algorithm is straight forward and given as a flow chart in Section 6.3.

It has to be called at the desired frequency to account for stability, speed and accuracy of the CFD simulation. After the CFD simulation is done, the light flux has to be corrected to the effective light flux with PWM signal, to obtain the actual light flux recognized by the LED user,

$$\Phi_{\mathrm{v,\,eff}} = f_{\mathrm{PWM}} \cdot \Phi_{\mathrm{v}}.$$

4.6 CFD result

We chose a generic setup to present the application of our LED model within CFD. The setup consists of a low power LED on a free floating FR4 type PCB surrounded by a box with heat transfer at fixed ambient temperature. The LED geometry is according to the description in Section 4.1. The horizontally aligned PCB has a thickness of 2 mm. Its surface area is $34 \times 33.7\ \mathrm{mm}^2$. The conduction layer of copper is accounted for with a thickness of 35 µm covering all the PCB. An overview is given in the upper left of Figure 11.

Two unsteady simulations were done at different boundary and initial conditions, see Table 1. The time step size was 1 s and the total simulation time is half an hour. In the upper side of Figure 11 it is shown the temperature distribution at the end of the simulation in a section in the LED symmetry for the first unsteady simulation. One can see the die as hottest place and lower temperatures at the solder position according to the right side of Figure 10. The temperature difference is defined by the thermal resistance and the thermal power according to equation (11) and fits the expectation well.

Table 1: Simulation settings.

Condition	Simulation 01	Simulation 02
$T_{\mathrm{amb}}/T_{\mathrm{typ}}$	3.2	4.0
$I_{\mathrm{F}}/I_{\mathrm{F,typ}}$	1.07	1.29
T_{j} control	No	$T_{\mathrm{j}}/T_{\mathrm{j,typ}} = 4.6$

The LED results are shown in the lower side of Figure 11. Each dot indicates the state at a time step. The current was set to $I_{\mathrm{F}}/I_{\mathrm{F,\,typ}} = 1.07$ and $I_{\mathrm{F}}/I_{\mathrm{F,\,typ}} = 1.29$, respectively. While time stepping the system heats up and the resulting state evolves toward higher temperature at a constant forward current. For the first simulation with the higher current the LED becomes so hot that the extrapolation region is reached which prevents the system to run into a non-physical state.

For the second simulation a controller was implemented in order to limit the temperature by reducing the forward current. This is seen in the green trace. The system heats up and reaches the limit temperature. The controller gets activated and, with a little delay, reduces the forward current so that the thermal equilibrium results in the limit temperature. Due to the small size of the system the temperature dynamics is high and there are no big oscillations occurring during the control process.

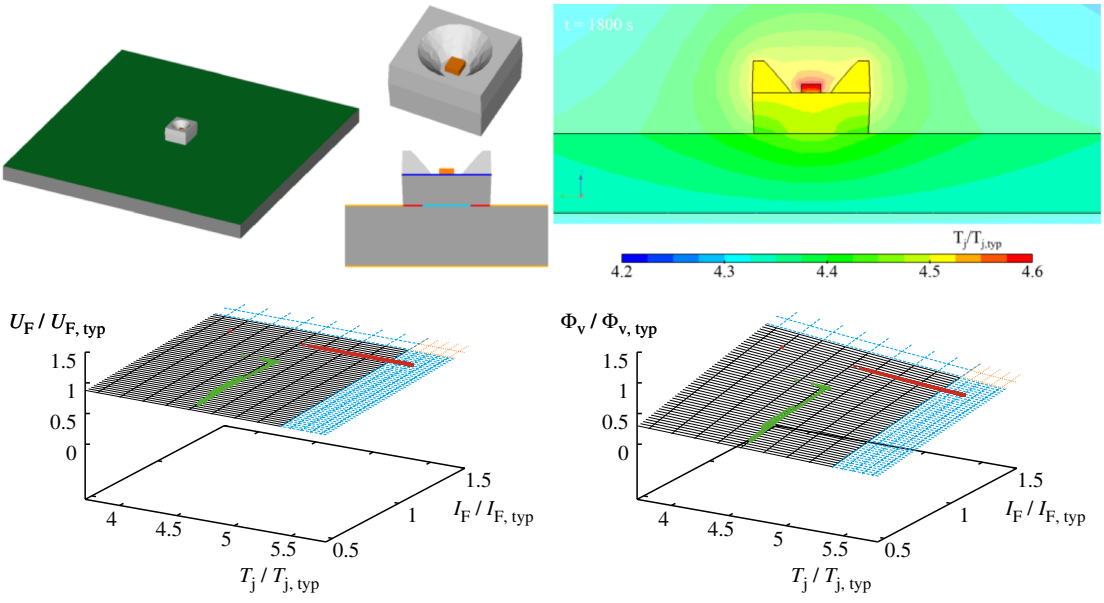

Figure 11: Overview of the CFD model (upper left) and its temperature distribution (upper right). Result in space of characteristics in the lower row; green: high temperature, $T_{\mathrm{j}}/T_{\mathrm{j,\,typ}}$=4 and $I_{\mathrm{F}}/I_{\mathrm{F,\,typ}}$=1.07, controlled to limit the junction temperature to $T_{\mathrm{j}}/T_{\mathrm{j,\,typ}}$=4.6; red: high temperature, $T_{\mathrm{j}}/T_{\mathrm{j,\,typ}}$=4 and $I_{\mathrm{F}}/I_{\mathrm{F,\,typ}}$=1.29.

5 Conclusions

With a rising number of LED manufacturers also the diversity of LED data sheets becomes larger. Technical data is provided at a variety of typical values, units and outputs, which makes it very difficult to compare LEDs of different manufacturers and to use the given data in simulations to determine the thermal status of the LED in different states.

In the present manuscript in Section 3 a generalized LED model was developed to overcome these difficulties and to get use out of the data given in the different data sheets. In Section 4 it is shown, how to expand the model to a variety of other technical values of interest and how to apply the resulting LED model in CFD simulations to successfully predict a thermal status of an LED in an arbitrary setting.

It has to be pointed out that the data inside the LED data sheets may contain measurements of different quality, see Section 2.3.1. With the presented LED model, these values will be taken as a basis and will not be checked further. But even if some measurements can have a lower quality, this way of using the values from the data sheets is the best one can do without undertake measurements for all used LEDs. The authors see great potential by using this generalized model to enhance the usability of technical values given by LED manufacturers and to enable time dependent CFD simulations even though resolving a LED in detail is not possible in an acceptable computing time.

Author contributions: All the authors have accepted responsibility for the entire content of this submitted manuscript and approved submission.
Research funding: None declared.
Conflict of interest statement: The authors declare no conflicts of interest regarding this article.

Appendix A – LED model

Calculation of regression coefficients based on T_j and I_F

I_F and T_j are given in a definition interval according to data sheet. We will span a two dimensional surface of at least two perpendicular curves according to Figures 7 and 8. Consider the following according to Section 2.3.2:

$U_F(T_j, I_F)$ add two graphs
$\phi_{rel}(T_j, I_F)$ multiply two graphs
$\Delta x(T_j, I_F)$ add two graphs
$\Delta y(T_j, I_F)$ add two graphs.

We perform the regression using a least squares approximation. Let us assume we have a set of points in two variables (x_i, y_i, z_i) for $i = 1,\ldots,n$. Let r be the polynomial order in x-direction and s the order in y-direction. By setting

$$r_i = z_i - \sum_{v=0}^{r}\sum_{w=0}^{s} \alpha_{vw} x_i^v y_i^w$$

for every $i = 1,\ldots,n$ we want to minimize

$$Q(\alpha) = \sum_{i=1}^{n} r_i^2 = \sum_{i=1}^{n} \left(z_i - \sum_{v=0}^{r}\sum_{w=0}^{s} \alpha_{vw} x_i^v y_i^w \right)^2.$$

The expression Q can be formulated with the help of the $n \times (r+1)(s+1)$-dimensional matrix X and the two vectors

$$X = \begin{pmatrix} 1 & x_1 & y_1 & x_1y_1 & \cdots & x_1^r y_1^s \\ 1 & x_2 & y_2 & x_2y_2 & \cdots & x_2^r y_2^s \\ \vdots & \vdots & \vdots & \vdots & & \vdots \\ 1 & x_n & y_n & x_ny_n & \cdots & x_n^r y_n^s \end{pmatrix},$$

$$\alpha = \begin{pmatrix} \alpha_{00} & \alpha_{10} & \alpha_{01} & \alpha_{11} & \cdots & \alpha_{rs} \end{pmatrix}^T,$$

$$z = \begin{pmatrix} z_1 & \cdots & z_n \end{pmatrix}^T$$

via

$$Q(\alpha) = (z - X\alpha)^T (z - X\alpha).$$

We aim to derive α from the minimization problem $Q(\alpha) \stackrel{!}{=} \min$. Hence, we solve $\partial/\partial\alpha_{ij} Q(\alpha) = 0$ and obtain

$$Q'(\alpha) = -2X^T (z - X\alpha) \stackrel{!}{=} 0.$$

The solution α satisfies

$$X^T X\alpha = X^T z.$$

This enables us to get

$$\alpha = \left(X^T X\right)^{-1} \left(X^T z\right),$$

if the $((r+1)(s+1))^2$-dimensional matrix $X^T X$ is invertible.

In practice, the LED suppliers give only two measured graphs. This is not enough to derive these full representations in Figures 7 and 8. By using only the two graphs, the regression polynomial oscillates heavily towards the boundaries. To avoid this physically unlikely behaviour, we use superposition to expand the given point set from the supplier linearly throughout the "black area" in the referenced figures.

Physical basis of characteristics

Electric characteristics

The I–U-characteristic of an idealized diode was found by William Shockley of Bell Telephone Laboratories in 1949, [5, 10]. It is an exponential dependency of forward current I_F on forward voltage U_F,

$$I_F = I_S\left(\exp\left(\frac{U_F}{nU_T}\right) - 1\right). \tag{19}$$

Herein, n is the emission coefficient and U_T the thermal voltage. The details are depending on the certain compound of the semiconductor materials forming the junction and not of importance for the further discussion because the characteristic is usually provided by the LED manufacturers, see upper left of Figure 4 for a red low power LED. These characteristics are usually obtained by measurements done by LED manufacturers.

The thermal voltage $U_T = k_B T_j/q$ relates the kinetic energy of the charges to the potential energy of the total charge q of the P–N-junction. This temperature dependence of the forward voltage is also provided by the manufacturers; see upper right of Figure 4 for the same red LED. The voltage difference, $\Delta U_F = U_F - U_{F,\,typ}$, is based on a typical voltage, $U_{F,\,typ}$, which is explained Section 3.

Luminous characteristics

Prerequesite for efficient light emission is a high probability of radiating recombinations within the P–N-junction, [11]. This is usually the case in semiconductor materials with a direct band gap, e.g. GaAs. The wave length λ of the emitted radiation depends on the energy difference, E_g, between valence band and conduction band

$$\lambda = \frac{h \cdot c}{E_g}. \tag{20}$$

It forms a distribution, as can be seen as red curve in Figure 1 for the red LED. The half width and the peak wave length of the spectrum depend, among others, on the temperature. The band gap and thus the energy of emitted photons sink with rising temperature. According to [4] this behaviour was found to be approximately linear for junction temperatures above 290 K according to Varshni formula

$$E_g(T_j) \approx E_{g,\,ref} - \alpha'(T_j - T_{ref}). \tag{21}$$

This leads to larger wave lengths and thus to a kind of redshift of the colour of the direct radiation as seen in Figure 5.

Extrapolations

Regression can only be done within the interval of data. If temperature or current outside this interval are used or reached there still shall exist a physically appropriate solution. Thus an extrapolation will be necessary. Let Ω be the domain of definition for the functions of interest according to equations (7) to (10).

Around the rectangular area Ω eight regions appear as can be seen in Figure 9. First we take the vertical and horizontal parts Ω_T-, Ω_T+, Ω_I- and Ω_I+.

Extrapolation of voltage

We take equation (7) and calculate the derivative with respect to T_j and I_F

$$\frac{\partial U_F(T_j, I_F)}{\partial I_F} = \sum_{i=0}^{n}\sum_{k=0}^{m} kc_{U,ik} \cdot T_j^i \cdot I_F^{k-1} \tag{22}$$

$$\frac{\partial U_F(T_j, I_F)}{\partial T_j} = \sum_{i=0}^{n}\sum_{k=0}^{m} ic_{U,ik} \cdot T_j^{i-1} \cdot I_F^{k}. \tag{23}$$

We use the following physically motivated functions.

– In Ω_{T-} we perform a linear ansatz $m \cdot x + a$ and for every $(T, I) \in \Omega_{T-}$ we find

$$\frac{\partial U_F(T_{j,min}, I_F)}{\partial T_j} \cdot (T_j - T_{j,min}) + U(T_{j,min}, I_F).$$

– In Ω_{T+} we use an exponential ansatz $a \cdot e^{b/x}$ and find for every $(T_j, I_F) \in \Omega_{T+}$

$$\frac{U_F(T_{j,max}, I_F)}{e^f} \cdot e^f$$

with

$$f = \frac{\frac{\partial}{\partial T_j} U(T_{j,max}, I_F)}{U(T_{j,max}, I_F)} T_{j,max}.$$

– In Ω_{I-} we do exponential extrapolation $a \cdot e^{b/x}$ until zero $I_F = 0$ and find for all $(T_j, I_F) \in \Omega_{I-}$

$$U_F(T_j, I_{F,min}) \cdot e^{f_1} \cdot e^{f_2}$$

with

$$f_1 = \frac{\frac{\partial}{\partial I_F} U_F(T_j, I_{F,min})}{U_F(T_j, I_{F,min})} I_{F,min}$$

and

$$f_2 = -\frac{\frac{\partial}{\partial I_F} U_F(T_j, I_{F,min})}{U_F(T_j, I_{F,min})} \frac{(I_{F,min})^2}{I_F}.$$

– In Ω_{I+} we do exponential extrapolation $a \cdot e^{b/x}$ and find for all $(T_j, I_F) \in \Omega_{I+}$

$$\frac{U_F(T_j, I_{F,max})}{e^{f_1}} \cdot e^{f_2}$$

with

$$f_1 = \frac{\frac{\partial}{\partial I_F} U_F(T_j, I_{F,max})}{U_F(T_j, I_{F,max})} I_{F,max}$$

and

$$f_2 = \frac{\frac{\partial}{\partial I_F} U_F(T_j, I_{F,max})}{U_F(T_j, I_{F,max})} I.$$

The remaining areas $\Omega_{--/-+/+-/++}$ comprise two bounding areas which can be used for extrapolation directly.

As an example, we derive a value U at $(T, I) \in \Omega_{++}$. From the extrapolated areas above we can observe that $U_{\mathrm{maxmax}} = U(T_{\mathrm{j,max}}, I_{\mathrm{F,max}})$, $U_{\mathrm{I\,max}} = U(T, I_{\mathrm{F,max}})$, and $U_{\mathrm{T\,max}} = U(T_{\mathrm{j,max}}, I)$ from Ω_I+ resp. Ω_T+ and the desired value via

$$U(T, I) = U_{\mathrm{maxmax}} + [U_{I\,\mathrm{max}} - U_{\mathrm{maxmax}}] + [U_{T\mathrm{max}} - U_{\mathrm{maxmax}}].$$

Extrapolation light flux

We take equation (8) and calculate the derivative with respect to T_j and I_F

$$\frac{\partial \Phi_{\mathrm{rel}}(T_\mathrm{j}, I_\mathrm{F})}{\partial I_\mathrm{F}} = \sum_{i=0}^{n}\sum_{k=0}^{m} kc_{\Phi,ik} \cdot T_\mathrm{j}^i \cdot I_\mathrm{F}^{k-1} \tag{24}$$

$$\frac{\partial \Phi_{\mathrm{rel}}(T_\mathrm{j}, I_\mathrm{F})}{\partial T_\mathrm{j}} = \sum_{i=0}^{n}\sum_{k=0}^{m} ic_{\Phi,ik} \cdot T_\mathrm{j}^{i-1} \cdot I_\mathrm{F}^{k}. \tag{25}$$

We use the following extrapolations motivated by physics.

– In Ω_{T-} we do linear extrapolation $m \cdot x + b$ and find for every $(T_\mathrm{j}, I_\mathrm{F}) \in \Omega_{T-}$

$$\frac{\partial}{\partial T_\mathrm{j}}\Phi_{\mathrm{rel}}(T_{\mathrm{j,min}}, I_\mathrm{F}) \cdot (T_\mathrm{j} - T_{\mathrm{j,min}}) + \Phi_{\mathrm{rel}}(T_{\mathrm{j,min}}, I_\mathrm{F}).$$

– In Ω_{T+} we apply an exponential extrapolation $a \cdot \mathrm{e}^{b/x}$ and get for every $(T_\mathrm{j}, I_\mathrm{F}) \in \Omega_{T+}$

$$\frac{\Phi_{\mathrm{rel}}(T_{\mathrm{j,max}}, I_\mathrm{F})}{\mathrm{e}^{f_1}} \cdot \mathrm{e}^{f_2}$$

with

$$f_1 = \frac{\frac{\partial}{\partial T_\mathrm{j}}\Phi_{\mathrm{rel}}(T_{\mathrm{j,max}}, I_\mathrm{F})}{\Phi_{\mathrm{rel}}(T_{\mathrm{jmax}}, I_\mathrm{F})} T_{\mathrm{j,max}}$$

and

$$f_2 = \frac{\frac{\partial}{\partial T_\mathrm{j}}\Phi_{\mathrm{rel}}(T_{\mathrm{j,max}}, I_\mathrm{F})}{\Phi_{\mathrm{rel}}(T_{\mathrm{j,max}}, I_\mathrm{F})} T_\mathrm{j}.$$

– In Ω_{I-} we perform an exponential extrapolation $a \cdot \mathrm{e}^{b/x}$ up to $I_\mathrm{F} = 0$, and get for every $(T_\mathrm{j}, I_\mathrm{F}) \in \Omega_{I-}$

$$\Phi_{\mathrm{rel}}(T_\mathrm{j}, I_{\mathrm{F,min}}) \cdot \mathrm{e}^{f_1} \cdot \mathrm{e}^{f_2}$$

with

$$f_1 = \frac{\frac{\partial}{\partial I_\mathrm{F}}\Phi_{\mathrm{rel}}(T_\mathrm{j}, I_{\mathrm{F,min}})}{\Phi_{\mathrm{rel}}(T_\mathrm{j}, I_{\mathrm{F,min}})} I_{\mathrm{F,min}}$$

and

$$f_2 = -\frac{\frac{\partial}{\partial I_\mathrm{F}}\Phi_{\mathrm{rel}}(T_\mathrm{j}, I_{\mathrm{F,min}})}{\Phi_{\mathrm{rel}}(T_\mathrm{j}, I_{\mathrm{F,min}})} \frac{(I_{\mathrm{F,min}})^2}{I_\mathrm{F}}.$$

– In Ω_{I+} we perform an extrapolation with the approach $A\sqrt{(x)} + b$ and we find for every $(T, I) \in \Omega_{I+}$

$$2\frac{\partial}{\partial I_\mathrm{F}}\Phi_{\mathrm{rel}}(T_\mathrm{j}, I_{\mathrm{F,max}}) \cdot \sqrt{I_{\mathrm{F,max}}} \cdot \left(\sqrt{I_\mathrm{F}} - \sqrt{I_{\mathrm{F,max}}}\right) + \Phi_{\mathrm{rel}}(T_\mathrm{j}, I_{\mathrm{F,max}}).$$

The other domains $\Omega_{--/-+/+-/++}$ are treated the same as in the previous part on the voltage U.

The extrapolation of the colours like shown in Figure 8 is treated only with linear extrapolation. Otherwise, they are derived in the same way as the values above.

Calculation algorithm

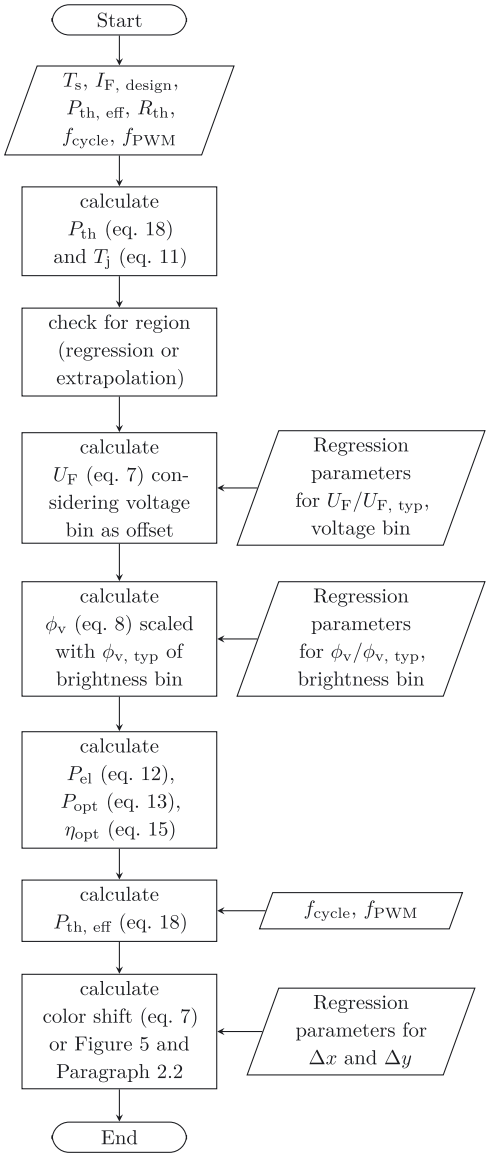

References

[1] K. Baran, M. Leśko, H. Wachta, and A. Różowicz, "Thermal modeling and simulation of high power led module," in *AIP Conference Proceedings*, 2019, p. 2078.

[2] H. M. Choi, L. Wang, S. Kang, J. Lim, and J. Choi, "Precise measurement of junction temperature by thermal analysis of light-emitting diode operated at high environmental temperature," *Microelectron. Eng.*, vol. 235, p. 111451, 2021.

[3] A. M. Colaco, C. P. Kurian, S. G. Kini, S. G. Colaco, and C. Johny, "Thermal characterization of multicolour led luminaire," *Microelectron. Reliab.*, vol. 78, pp. 379–388, 2017.

[4] A. Keppens, "Modelling and Evaluation of High-Power Light-Emitting Diodes for General Lighting," Ph.D. Thesis Light and Lighting Laboratory Gent, 2010.

[5] C. Kittel, *Introduction to Solid State Physics*, 8th ed. New York, NY, John Wiley and Sons, Inc, 2004.

[6] D. Lee, H. Choi, S. Jeong, et al., "A study on the measurement and prediction of LED junction temperature," *Int. J. Heat Mass Transfer*, vol. 127, pp. 1243–1252, 2018.

[7] Y. Ohno, "Cie fundamentals for colour measurements," in *Digital Printing Technologies; IS&T's NIP16, International Conference, CA, No. 16*, 2000.

[8] A. Poppe, "Multi-domain compact modeling of leds: an overview of models and experimental data," *Microelectron. J.*, vol. 46, pp. 1138–1151, 2015.

[9] A. Poppe, "Simulation of led based luminaires by using multi-domain compact models of leds and compact thermal models of their thermal environment," *Microelectron. Reliab.*, vol. 72, pp. 65–74, 2017.

[10] W. Shockley, "The theory of p–n junctions in semiconductors and p-n junction transistors," *Bell Syst. Tech. J.*, vol. 28, no. 3, pp. 435–489, 1949.

[11] F. Thuselt, *Physik der Halbleiterbauelemente. 2. Auflage*, Heidelberg, Springer, 2011.

[12] L. Yang, S. Jang, W. Hwang, and M. Shin, "Thermal analysis of high power gan-based leds with ceramic package," *Thermochim. Acta*, vol. 455, pp. 95–99, 2007.